Penerbit Akademia Baru

CFD Letters

Journal homepage: www.akademiabaru.com/cfdl.html
ISSN: 2180-1363

Development of Performance Correlations using ACFD Method for 2-D Curved Diffuser

Open Access

Muhammad Zahid Firdaus Shariff[1], Normayati Nordin[1,*], Lim Chia Chun[1], Shamsuri Mohamed Rasidi[1], Raudhah Othman[1], Sharifah Adzila[1]

[1] Faculty of Mechanical and Manufacturing Engineering, Universiti Tun Hussein Onn Malaysia, 86400 Batu Pahat, Johor, Malaysia

ARTICLE INFO

Article history:
Received 20 June 2020
Received in revised form 19 August 2020
Accepted 24 August 2020
Available online 30 August 2020

ABSTRACT

Diffuser is a fluid mechanical device which allows the recovery of pressure energy from the fluid flow on the outlay of kinetic energy. Performance of turning diffuser is evaluated primarily by pressure recovery coefficient, C_p and flow uniformity, σ_{out}. The varying of geometrical and operating parameters could alter the performance of the diffuser. Hence, this study aims to investigate the effect of angle of turn, ϕ on 2-D curved diffuser performance and to develop performance correlations. The angle of turn was varied from 30° to 180°. The evaluation for performance of the curved diffusers was done by using ANSYS Fluent with the most appropriate turbulence model of Reynolds Stress Model (RSM) added with enhanced wall treatment of y^{+}=1.0. Performance correlations in terms of pressure recovery and flow uniformity were developed by implementing Asymptotic Computational Fluid Dynamics (ACFD) technique. Pressure recovery of the curved diffusers showed a declining pattern by approximately 79.5% while flow uniformity shows higher distortion up to 52.6% with the increase of angle of turn from 30° to 180°. Hence, it has been proven that the increase of angle of turn has affected the performance of curved diffuser significantly. The ACFD performance correlations has provided acceptable deviations to both CFD and experimental results.

Keywords:
2-D curved diffuser; angle of turn; pressure recovery coefficient; flow uniformity; Asymptotic Computational Fluid Dynamics (ACFD)

1. Introduction

Diffuser in its basic form is a straight duct with increased cross section at its outlet. This fluid mechanical device is largely used for its ability to recover pressure energy from the flowing fluid at the expense of fluid kinetic energy [1]. Diffusers are classified by their geometry and parameters which vary for each application. A straight diffuser has no angle of turn whereas a curved diffuser has certain angle of turn [2-3]. Curved diffusers are often introduced in HVAC systems [4], circulating fluidized bed (CFB) system [5], turbines [6-8], and wind tunnel system [9-10]. Many mechanical

* *Corresponding author.*
E-mail address: mayati@uthm.edu.my (Normayati Nordin)

https://doi.org/10.37934/cfdl.12.8.116

engineering systems such as inlet gates on dams, turbine, ducting systems and compressor cross-overs require the installation of diffuser to reduce the fluid flow velocity where the fluid is flowing around the bending ducts [11].

The performance of a diffuser is measured by its ability to recover pressure and the uniformity of flow at its outlet [2]. These indexes are greatly affected by the diffuser's geometry and operating parameters. Previous studies proved that the performance of a curved diffuser is affected by its degree of angle of turn [12]. Due to the curved geometry of a diffuser, the centrifugal force created inside it which results in flow separation would decrease the performance of a curved diffuser [13].

There are currently correlations for curved diffusers such as the work of Nordin *et al.,* [14] and Khong *et al*., [12] but it is not comprehensive enough to include angle variations from $30^{\circ}$to 180°. Thus, the objective of the current study is to evaluate numerically the effect of angle of turn on performance and develop the performance correlations of 2-D curved diffuser by varying the angle of turn from $30^{\circ}$to 180°.

2. Methodology

2.1 Performance Index

Performance of curved diffuser is defined by the:

(i) Pressure recovery coefficient, C_p

$$C_p = \frac{2(P_{outlet} - P_{inlet})}{\rho {V_{inlet}}^2} \quad (1)$$

Where,

P_{outlet} = Average static pressure located at diffuser outlet (Pa)
P_{inlet} = Average static pressure located at diffuser outlet (Pa)
ρ = Density of air (kg/m^3)
V_{inlet} = Inlet air mean velocity (m/s)

(ii) Flow uniformity index, σ_{out}

$$\sigma_{out} = \sqrt{\frac{1}{N-1}\sum_{i=1}^{N}(V_i - V_{out})^2} \quad (2)$$

Where,

N = Number of measurement points
V_i = Local outlet air velocity (m/s)
V_{out} = Mean outlet air velocity (m/s)

2.2 Modelling

The 2-D curved diffusers were modelled using Solidworks software. Five models of curved diffusers were constructed by varying the angle of turn, $\phi = 30^{\circ}, 90^{\circ}, 120^{\circ}, 150^{\circ}, 180^{\circ}$ as shown in Figure 1. The geometrical parameters of these 2-D curved diffusers are shown in Table 1 which

W_1 and X_1 are the height and width of diffuser inlet, W_2 and X_2 are the height and width of diffuser outlet, r_{in} is the inner circle radius, L_{in} is the inner wall length, r_m is the center circle radius, L_m is the center length of the diffuser, and L_e is the extended length of diffuser. Figure 2 shows the sketch of 90˚ curved diffuser with its construction lines and geometrical parameters.

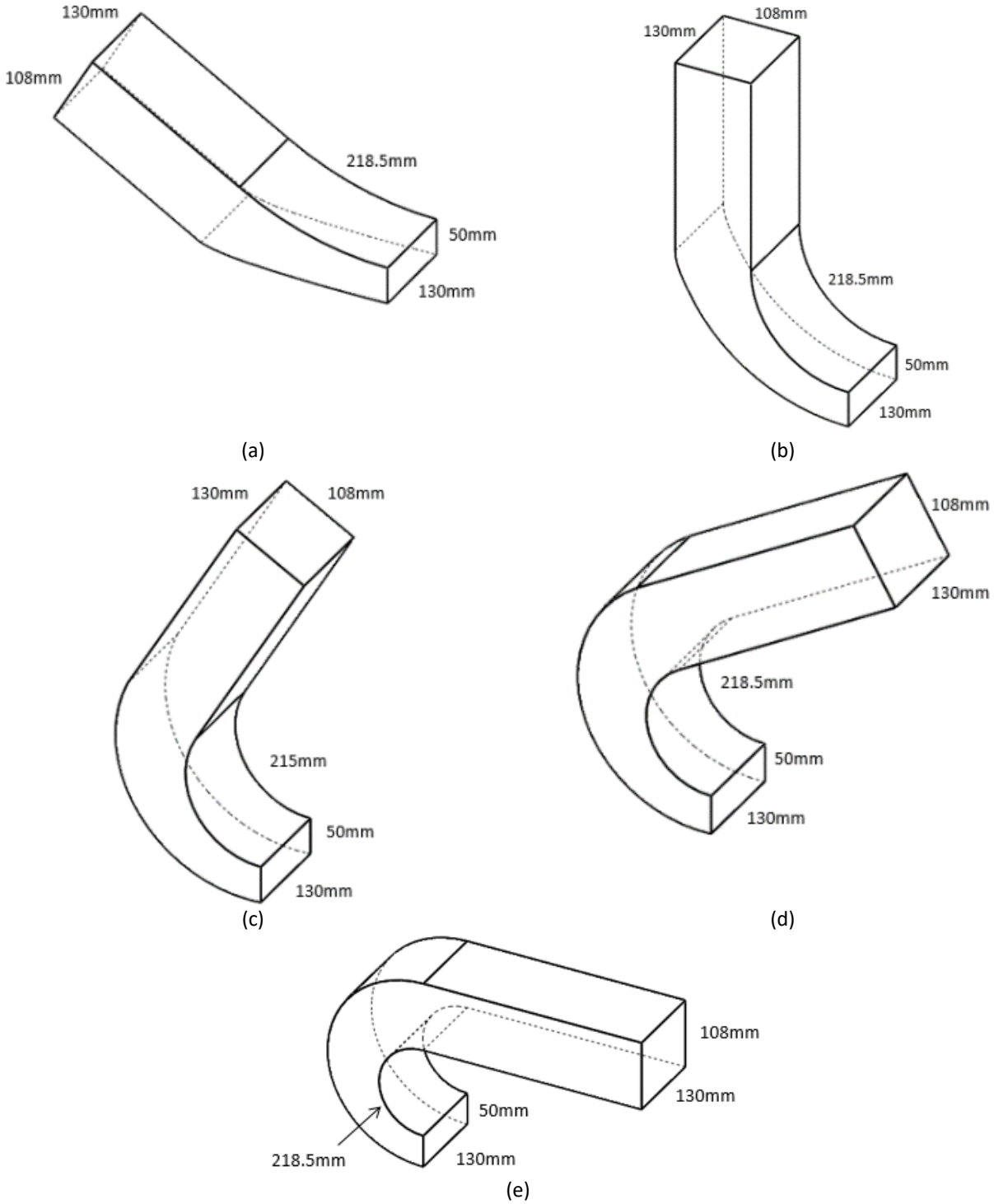

Fig. 1. 2-D curved diffuser models with turning angle of (a) $\phi_1 = 30^{\circ}$, (b) $\phi_2 = 90^{\circ}$, (c) $\phi_3 = 120^{\circ}$, (d) $\phi_4 = 150^{\circ}$, and (e) $\phi_5 = 180^{\circ}$

Table 1
Geometrical parameters of 2-D curved diffuser

ϕ	W_1	X_1	W_2	X_2	r_{in}	L_{in}	r_m	L_m	L_e
30°	50	130	108	130	417.30	218.50	755.72	239.11	239.11
90°	50	130	108	130	139.10	218.50	195.66	275.64	275.64
120°	50	130	108	130	104.33	218.50	144.95	300.56	300.56
150°	50	130	108	130	83.46	218.50	123.11	321.65	321.65
180°	50	130	108	130	69.55	218.50	109.05	342.38	342.38

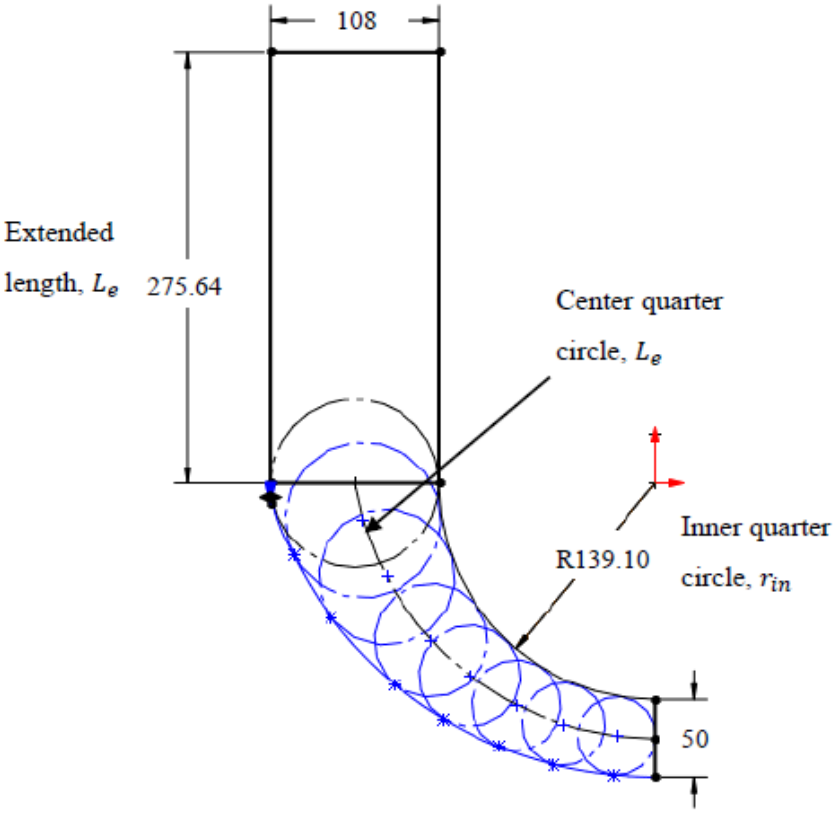

Fig. 2. Sketching and parameters of curved diffuser model

2.3 Meshing

Number of node and element could increase by reducing the element size and number of inflation layer. Skewness of the meshing must be less than 0.3. In fact, different meshing method could result in different cell structure. In the current study, the meshing was generated by using the method of Inflation and Multizone. Inflation meshing was implemented to set the first grid point off the wall which is 2.278×10^{-5}m. MultiZone was implemented to set the mapped mesh type into "Hexa" in order to produce Hexahedron cell structure of meshing. Figure 3 shows the mesh generated by using the method of Inflation and Multizone.

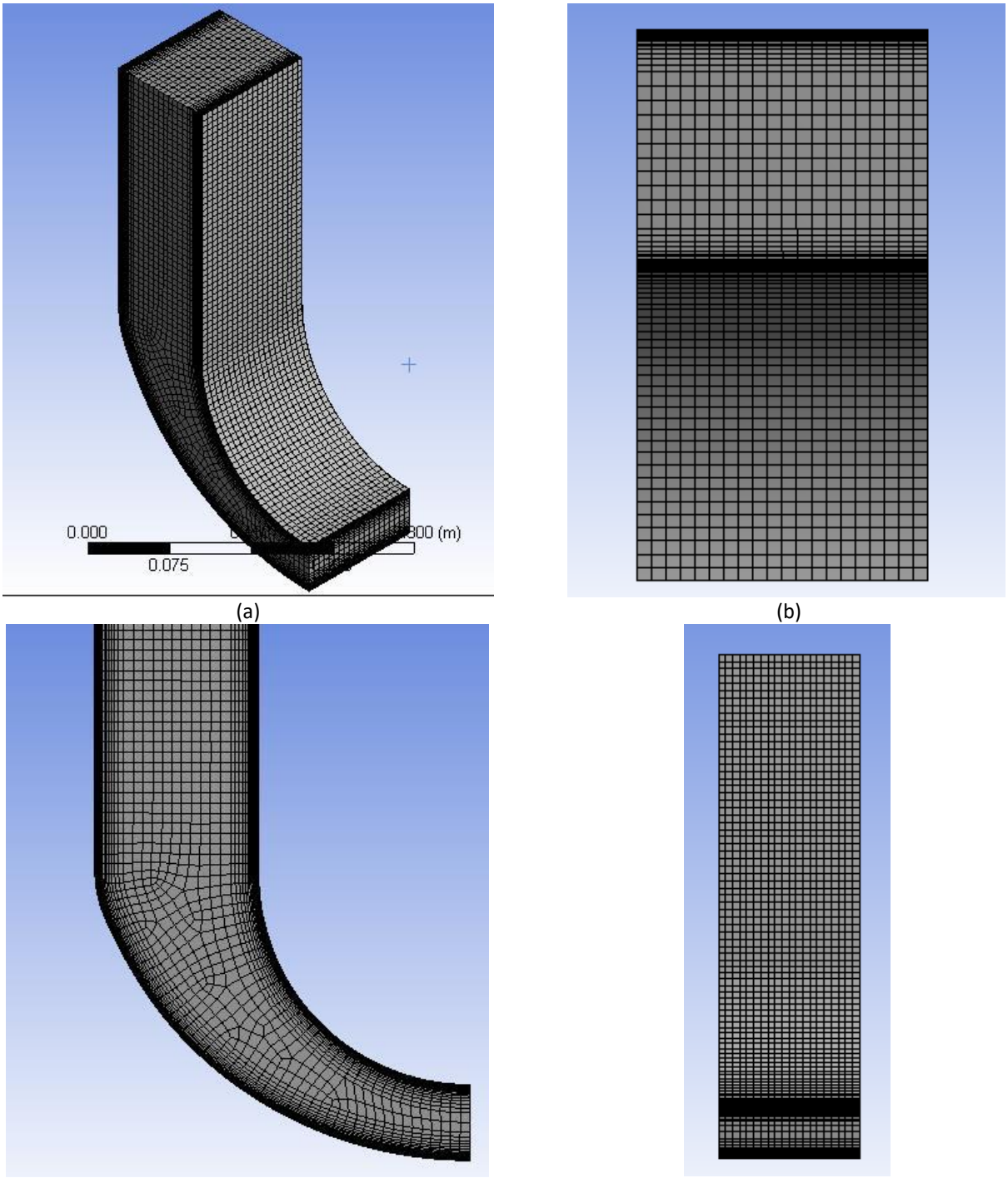

Fig. 3. Hexahedron cell structure of meshing (a) isometric view, (b) top view, (c) front view and (d) longitudinal view

2.4 Grid Independency Test

Grid independency test is a study of determining the appropriate mesh setting for the models created by running the simulation for each increase of nodes and elements. Mesh setting is refined as the number of nodes and elements increase until the simulation result shows an acceptable deviation percentage from two recent mesh setting. After consideration for accuracy and CPU solution time, the mesh with the lower number of nodes and elements between the two mesh

settings was chosen for the entire study. For this study, the mesh of curved diffuser was generated in Hexahedron cell structure.

2.5 Boundary Conditions

The boundary conditions for all boundary zones are set up according to Table 2. The diffuser inlet is set to have a velocity of 14.25 m/s, turbulent intensity of 4.0 % and hydraulic diameter 72.22 mm. The diffuser outlet is set to default pressure of 0 (atmospheric pressure). The walls of the diffuser are set to be in no slip shear condition. The working fluid is air with temperature of 30℃, density 1.164 $\mathrm{kg/m^3}$ and dynamic viscosity of 1.872×10^{-5} $\mathrm{kg/m.s}$.

Table 2
Boundary operating conditions for 2-D curved diffuser

Diffuser Inlet	Boundary type	Velocity-inlet
	Velocity magnitude, $V_{in}(m/s)$	14.25 ($Re_{in} = 6.385 \times 10^4$)
	Turbulent intensity, $I_{in}(\%)$	4.0
	Hydraulic diameter, $D_h(mm)$	72.22
Diffuser Outlet	Boundary type	Pressure-outlet
	Pressure (Pa)	0 (Atmospheric pressure)
Wall	Boundary type	Smooth wall
	Shear condition	No-slip
Working fluid properties	Working fluid	Air
	Temperature (℃)	30
	Density, ρ (kg/m^3)	1.164
	Dynamic viscosity, μ $(kg/m.s)$	1.872×10^{-5}

2.6 Governing Equations

The Reynolds-Averaged Navier-Stokes equation (RANS) is used to solve the analysis for Newtonian and incompressible fluid flow which is shown as following:

Continuity equation:

$$\frac{\partial u}{\partial x} + \frac{\partial v}{\partial y} + \frac{\partial w}{\partial z} = 0 \tag{3}$$

x-momentum equation:

$$u\frac{\partial u}{\partial x} + v\frac{\partial u}{\partial y} + w\frac{\partial u}{\partial z} = -\frac{1}{\rho}\frac{\partial P}{\partial x} + v\left[\frac{\partial^2 u}{\partial x^2} + \frac{\partial^2 u}{\partial y^2} + \frac{\partial^2 u}{\partial z^2}\right] + \frac{1}{\rho}\left[\frac{\partial(-\rho\overline{u'^2})}{\partial x} + \frac{\partial(-\rho\overline{u'v'})}{\partial y} + \frac{\partial(-\rho\overline{u'w'})}{\partial z}\right] \tag{4}$$

y-momentum equation:

$$u\frac{\partial v}{\partial x} + v\frac{\partial v}{\partial y} + w\frac{\partial v}{\partial z} = -\frac{1}{\rho}\frac{\partial P}{\partial y} + v\left[\frac{\partial^2 v}{\partial x^2} + \frac{\partial^2 v}{\partial y^2} + \frac{\partial^2 v}{\partial z^2}\right] + \frac{1}{\rho}\left[\frac{\partial(-\rho\overline{u'v'})}{\partial x} + \frac{\partial(-\rho\overline{v'^2})}{\partial y} + \frac{\partial(-\rho\overline{v'w'})}{\partial z}\right] \tag{5}$$

z-momentum equation:

$$u\frac{\partial w}{\partial x} + v\frac{\partial w}{\partial y} + w\frac{\partial w}{\partial z} = -\frac{1}{\rho}\frac{\partial P}{\partial z} + v\left[\frac{\partial^2 w}{\partial x^2} + \frac{\partial^2 w}{\partial y^2} + \frac{\partial^2 w}{\partial z^2}\right] + \frac{1}{\rho}\left[\frac{\partial(-\rho\overline{u'w'})}{\partial x} + \frac{\partial(-\rho\overline{v'w'})}{\partial y} + \frac{\partial(-\rho\overline{w'^2})}{\partial z}\right] \tag{6}$$

2.7 Solver

In order for simulations to have an accurate data, a suitable turbulence model should be chosen from several. Most common turbulence models were applied to determine the performance of turning diffuser namely Standard *k*-ε (ske) Turbulence Model, Shear Stress Transport $k-\omega$ (SST $k-\omega$) model and Reynolds Stress Model (RSM). Detail setting for the simulation of the curved diffusers in ANSYS CFD is shown in Table 3. The simulation applied the pressure-linked equation with semi-implicit method (SIMPLE). The SIMPLE algorithm was derived from the continuity and momentum equation combined in order to derive pressure equation. The Green-Gauss-Cell based was used to occupy the solution for the gradient while QUICK-type scheme was applied for the momentum equations, turbulent dissipation rate equation and turbulent kinetic energy equation. A convergence value of 10^{-5} was suggested as the residual error for all the governing equations in this study [15].

Table 3
Detail setting for the simulation of 2-D 90° curved diffuser in ANSYS Fluent

Mesh	
Type of Mesh	Hexahedron
Models	
Solver method	Reynolds Stress Model (RSM), Standard *k*-ε (ske), Shear Stress Transport $k-\omega$ (SST $k-\omega$)
Solution Methods	
Solver Scheme	SIMPLE
Gradient	Green-Gauss Cell Based
Pressure	PRESTO!
Momentum	QUICK
Turbulent Kinetic Energy	QUICK
Turbulent Dissipation Rate	QUICK
Reynolds Stresses	First order upwind

2.8 CFD Validation

The validation work is done by comparing the result from the experimental study by Nordin *et al.*, [2]. The focus of this validation is the pressure recovery performance, flow uniformity and flow structure. The curved diffuser geometry and operating parameters for validation work is shown in Table 4.

Table 4
Parameters of validation case [2]

Parameter	Magnitude
Re_{in}	6.382×10^4
W_2/W_1	2.16
L_{in}/W_1	4.37
X_2/X_1	1.00
ø	90°
C_p	0.209
σ_{out}	2.69

2.9 ACFD Method

The performance correlations for 2-D curved diffuser with varying angle of turn from 30° to 180° were developed by using the technique of Asymptotic Computational Fluid Dynamics (ACFD). The

main steps to develop the performance correlation for 2-D curved diffuser using ACFD technique are as follows [2,12,16]:

I. Identifying the dependent and independent variables
II. Linearizing the interconnection between dependent and independent variables
III. Employing the Taylor's series expansion
IV. Resolving convergence points and gradients
V. Substitutes all the constants

$C_{p\ acfd} = f\ (Re_{in}, W_2/W_1, L_{in}/W_1, \phi)$ (7)

$\sigma_{out\ acfd} = f\ (Re_{in}, W_2/W_1, L_{in}/W_1, \phi)$ (8)

$$\eta\ (\phi_1, \phi_2, \phi_3, \dots \phi_n) = \eta_{ref} + (\phi_1 - \phi_{1\,ref})\frac{\partial \eta}{\partial \phi_1} + (\phi_2 - \phi_{2\,ref})\frac{\partial \eta}{\partial \phi_2} + (\phi_3 - \phi_{3\,ref})\frac{\partial \eta}{\partial \phi_3} + \dots + (\phi_n - \phi_{n\,ref})\frac{\partial \eta}{\partial \phi_n} \quad (9)$$

Where,

η = dependent variables (C_p,σ_{out})

$\phi_1 = \left[\frac{Re_{in}}{Re_{in\,ref}}\right]^a$, $\phi_2 = \left[\frac{L_{in}/W_{in}}{L_{in}/W_{1\,ref}}\right]^b$, $\phi_3 = \left[\frac{W_2/W_1}{W_2/W_{1\,ref}}\right]^c$, and $\phi_4 = \left[\frac{\phi}{\phi_{ref}}\right]^d$

Where ϕ_1, ϕ_2, ϕ_3 and ϕ_4 represent the dimensionless independent group.

3. Result and Discussion

3.1 Grid Independency Test

The grid independence test was conducted by observing the pressure recovery, C_p value for the 2-D curved diffuser as the mesh is being refined in stages. The acceptable deviation of C_p between mesh settings is 5%. Thus, the mesh with lower deviation is chosen as the optimum mesh setting and used throughout this study. Table 5 shows the deviation between mesh 5 and 6 have a deviation for C_p of 6.63% while mesh 6 and 7 have a deviation of 1.32%. Mesh 7 with 363,965 elements was chosen as the optimum mesh setting instead of mesh 8 as the deviation between them is too small with increasing the solution time.

Table 5
Grid independency test for 90° 2-D curved diffuser

Mesh	Elements	Pressure Recovery, C_p	Deviation, %
1	107640	0.0447	53.58
2	158640	0.0963	39.43
3	213975	0.1590	11.86
4	262110	0.1804	10.11
5	304224	0.2007	6.92
6	327162	0.2156	6.63
7	363965	0.2309	1.32
8	386820	0.2340	-

3.2 CFD Validation Result

In order to obtain an accurate and reliable data, the result from CFD must undergo validation process with an experimental data, which in this study is the data from the experimental work by Nordin *et al.,* [2]. The values of pressure recovery, C_p obtained from the CFD simulations using three turbulence models are compared with the experimental data in Table 6. The turbulence model chosen to be used for intensive simulation is Reynolds Stress Model (RSM) which produced the result with the least and acceptable deviation of 10.47% compared to turbulence model Standard $k-\varepsilon$ and SST $k-\omega$. Figure 4 shows the velocity profile for the three turbulence models while Figure 5 shows the flow structure of experimental and RSM simulation result.

Table 6
Deviation of pressure recovery, C_p for different solver model with experimental result

Turbulence Model	Pressure recovery, C_p	Deviation (%)
Standard $k-\varepsilon$	0.2760	32.06
SST $k-\omega$	0.1744	16.56
RSM	0.2309	10.47
Experiment	0.2090	-

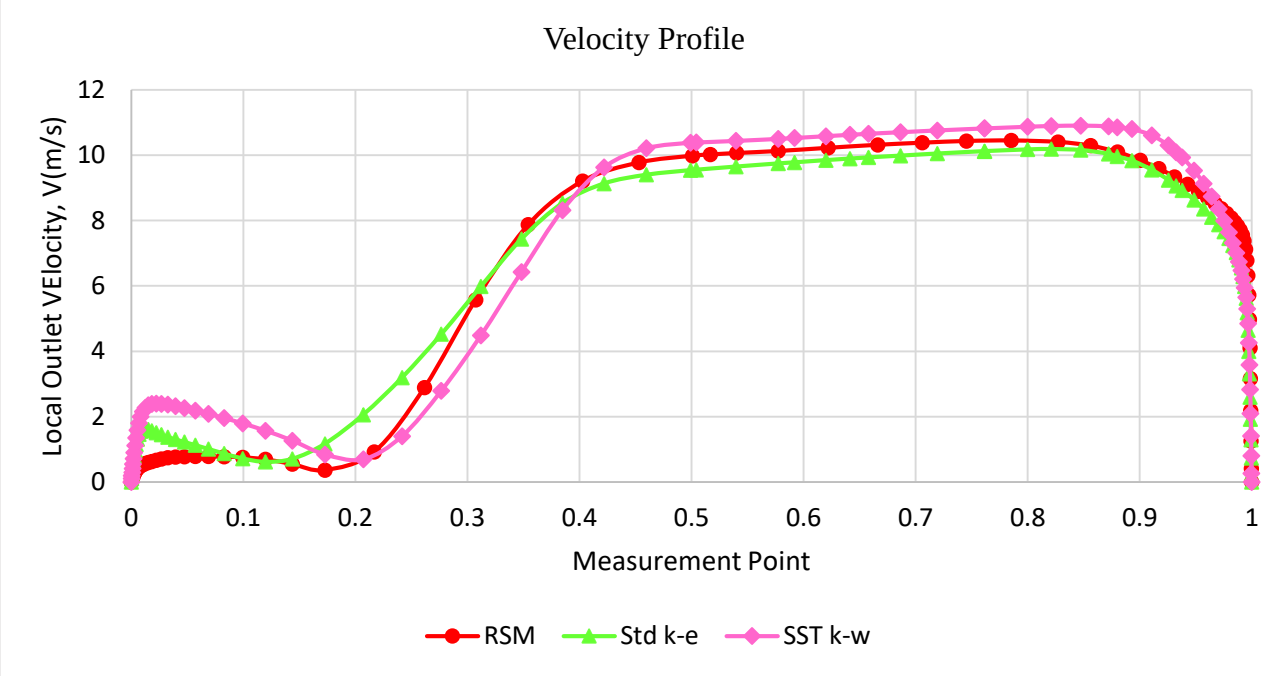

Fig. 4. Velocity profile for different solver models

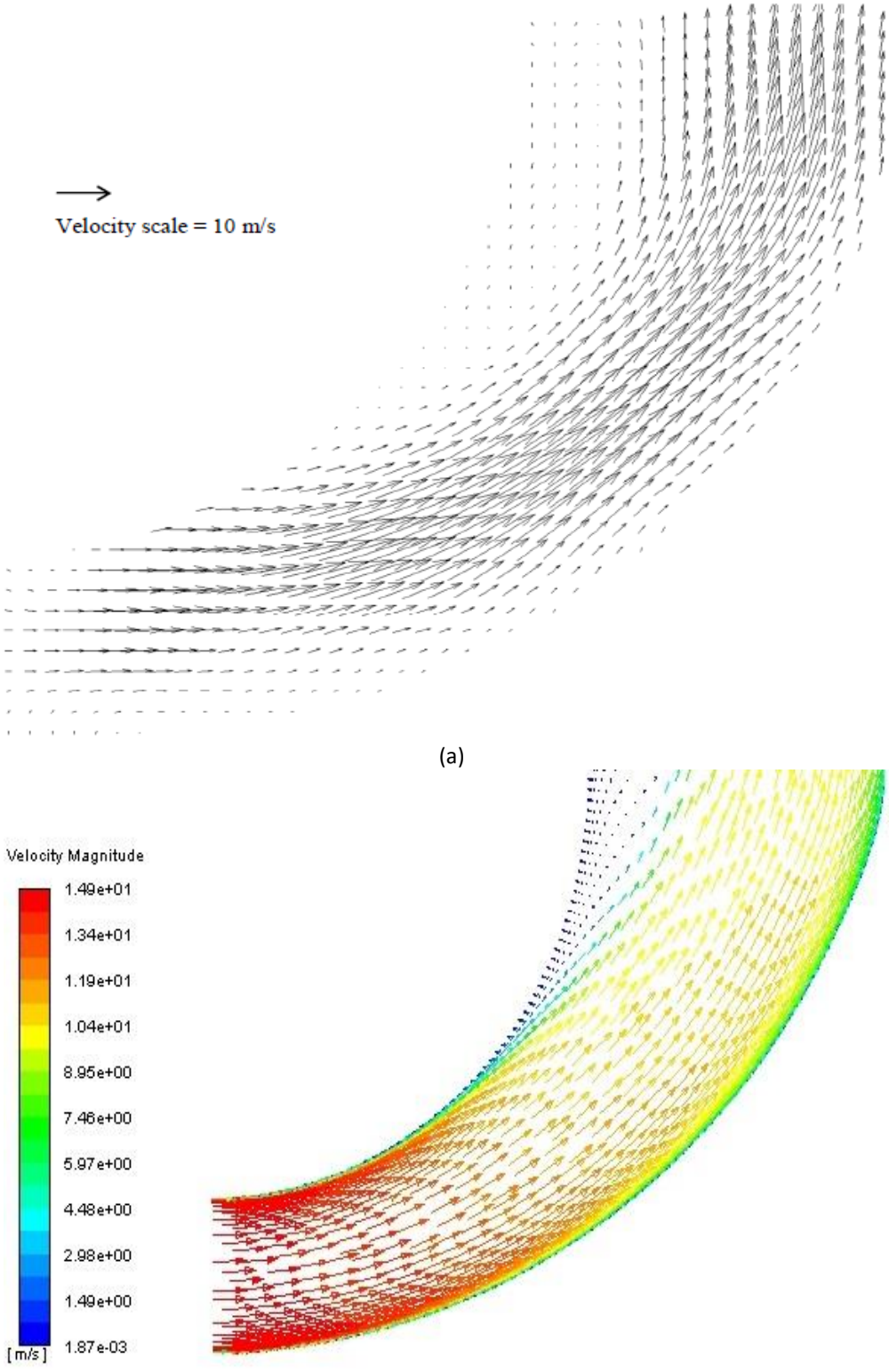

Fig. 5. Flow structure from (a) experimental result [2] and (b) RSM simulation result

3.3 Effect of Angle of Turn, ϕ

The results of pressure recovery, C_p, flow uniformity, σ_{out}, and flow separation point, S obtained from intensive simulation on the 2-D curved diffuser with varying angle of turn, ϕ is shown in Table

7. Higher value of C_p and lower value of σ_{out} indicates higher performance. The results prove that by increasing the angle of turn from $30^{\circ}$to 180°, the C_p decreases by approximately 79.5% and flow uniformity distorted by approximately 52.6%.

Figure 6 shows the velocity profiles for each 2-D curved diffuser from $30^{\circ}$to 180° angle of turn. The velocity profile gets less uniform and the flow concentrates more at the outer wall as the angle of turn increases. Due to the diffuser's geometry, the centrifugal force affects the fluid flow to lean towards the outer wall while creating flow separation at the inner wall. Figure 7 shows the flow separation caused a reverse flow near the inner wall of the diffuser. The separation point occurred nearer to the inlet of the diffuser as the angle of turn increases.

Table 7
Performance of 2-D curved diffuser by varying the turning angle from 30° to 180°

Turning angle, ϕ	Pressure recovery, C_p	Flow uniformity, σ_{out}	Flow separation point, S
30°	0.464	3.235	-
90°	0.231	3.823	0.646 L_1/W_1
120°	0.274	3.668	0.578 L_1/W_1
150°	0.109	4.936	0.404 L_1/W_1
180°	0.095	4.741	0.391 L_1/W_1

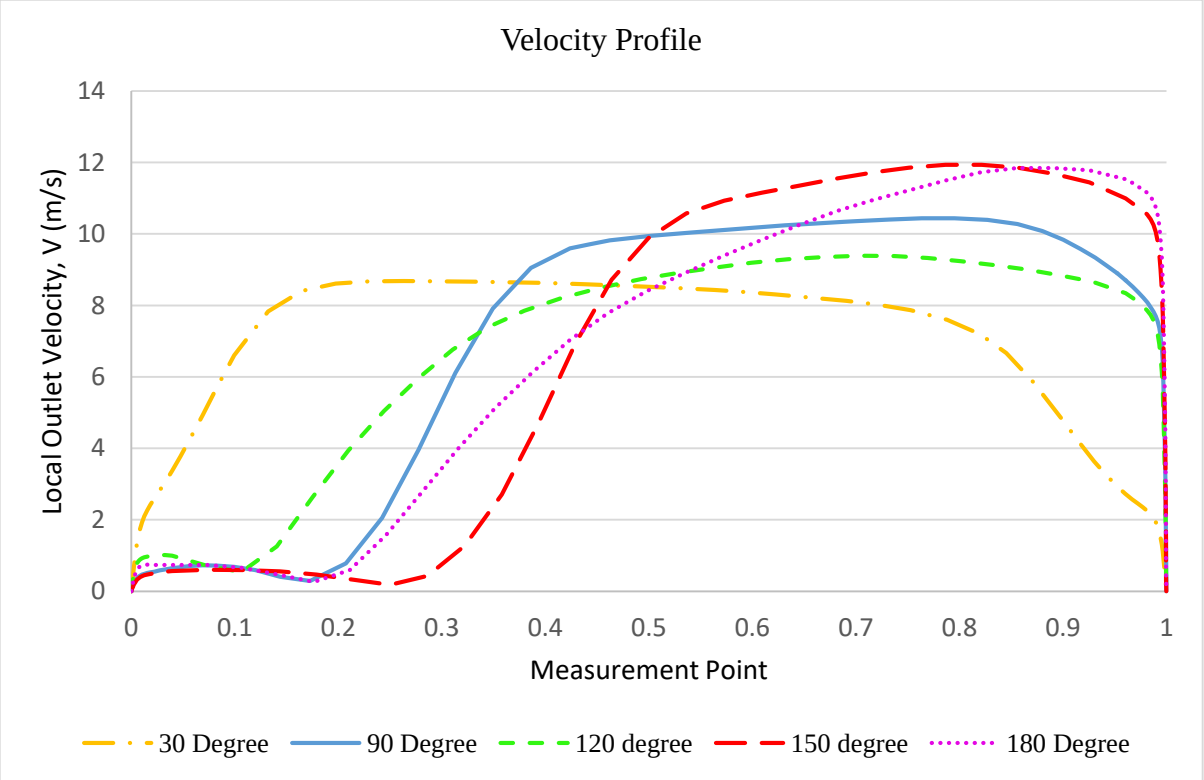

Fig. 6. Velocity profile of 2-D curved diffuser for turning angles 30°, 90°, 120°, 150° and 180°

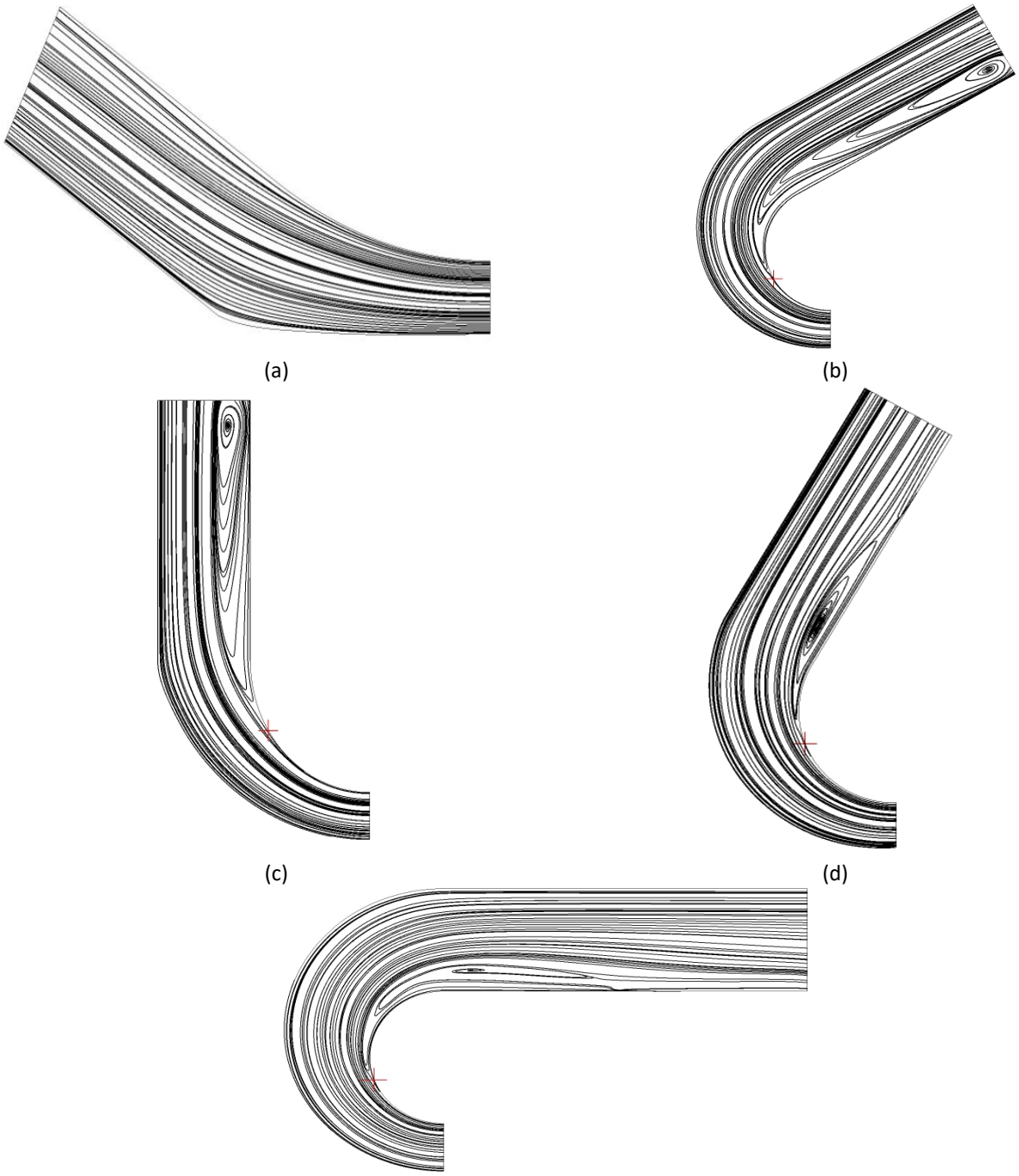

Fig. 7. Flow separation of 2-D curved diffuser for turning angles (a) 30°,(b) 90°, (c) 120°,(d) 150° and (e)180°

3.4 Development of ACFD Performance Correlations for 2-D Curved Diffuser

Correlation of two-dimensional (2-D) turning diffuser, $C_{p\,acfd}$ are develop by employing Taylor series expansion.

$$C_{p\,acfd} = C_{p\,ref} + \left(\emptyset_1 - \emptyset_{1\,ref}\right)\frac{\partial C_p}{\partial \emptyset_1} + \left(\emptyset_2 - \emptyset_{2\,ref}\right)\frac{\partial C_p}{\partial \emptyset_2} + \left(\emptyset_3 - \emptyset_{3\,ref}\right)\frac{\partial C_p}{\partial \emptyset_3} + \left(\emptyset_4 - \emptyset_{4\,ref}\right)\frac{\partial C_p}{\partial \emptyset_4} \quad (10)$$

$$\emptyset_1 = \left[\frac{Re_{in}}{Re_{in\,ref}}\right]^a, \emptyset_2 = \left[\frac{L_{in}/W_1}{L_{in}/W_{1\,ref}}\right]^b, \emptyset_3 = \left[\frac{W_2/W_1}{W_2/W_{1\,ref}}\right]^c \text{ and } \emptyset_4 = \left[\frac{\emptyset}{\emptyset_{ref}}\right]^d$$

Where $\emptyset_1, \emptyset_2, \emptyset_3$ and $\emptyset_4$ are dimensionless independent groups.

The values of a=1, b=1.5, c=2 and d=0.4 were determined in order to fit all the trend-lines in a graph and coincide at point $C_{p\,ref}$= 0.20 as shown in Figure 8. The inter-relations of dependent variable of C_p with each independent variable were linearized to obtain the best fit straight line.

$$\emptyset_{1\,ref} = \left[\frac{Re_{in\,ref}}{Re_{in\,ref}}\right]^a = 1.0,$$

Therefore, $\emptyset_{2\,ref} = \emptyset_{3\,ref} = \emptyset_{4\,ref} = 1.0$ as well. $\frac{\partial C_p}{\partial \emptyset_1} = 0.0215$, $\frac{\partial C_p}{\partial \emptyset_2}$ =-0.2998, $\frac{\partial C_p}{\partial \emptyset_3} = -0.013$, and $\frac{\partial C_p}{\partial \emptyset_4}$ =-0.5444 represented the slopes of the corresponding lines.

All the constants obtained are substituted into Eq. (10) yielding,

$$C_{p\,acfd} = 0.20 + \left(\left[\frac{Re_{in}}{Re_{in\,ref}}\right]^1 - 1\right)0.0215 - \left(\left[\frac{L_{in}/W_1}{L_{in}/W_{1\,ref}}\right]^{1.5} - 1\right)0.2998 - \left(\left[\frac{W_2/W_1}{W_2/W_{1\,ref}}\right]^2 - 1\right)0.013 - \left(\left[\frac{\emptyset}{\emptyset_{ref}}\right]^{0.4} - 1\right)0.5444 \quad (11)$$

Where,

$Re_{in\,ref} = 6.382 \times 10^4$, $L_{in}/W_{1\,ref}$ = 4.37, $W_2/W_{1\,ref}$ = 1.2 and $\emptyset_{ref} = 90^\circ$

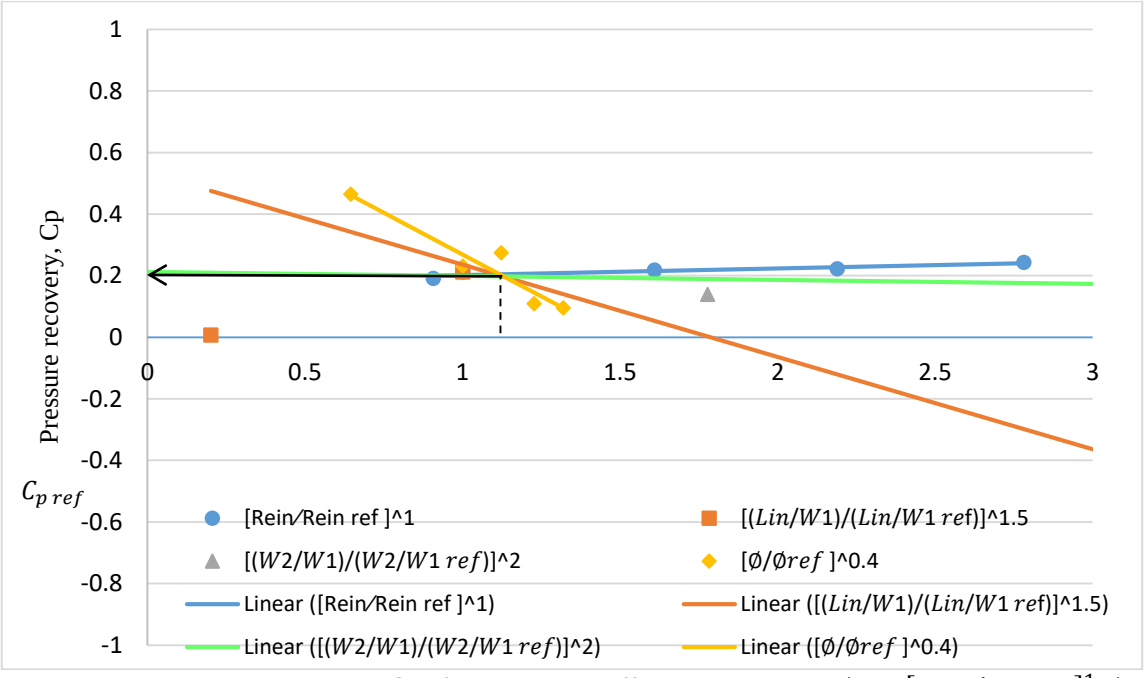

Fig. 8. Outlet pressure recovery, C_p of 2-D turning diffuser relatives to $\emptyset_1 = [\mathrm{Re_{in}/Re_{in\,ref}}]^1$,$\emptyset_2 = [\mathrm{L_{in}/W_1/L_{in}/W_{1\,ref}}]^{1.5}$, $\emptyset_3 = [\mathrm{W_2/W_1/W_2/W_{1\,ref}}]^2$ and $\emptyset_4 = [\emptyset/\emptyset_{\mathrm{ref}}]^{0.4}$

The correlation of flow uniformity, σ_{out} for two-dimensional turning diffuser was also developed by applying Taylor series expansion as well.

$$\sigma_{out\,acfd} = \sigma_{out\,ref} + \left(\emptyset_1 - \emptyset_{1\,ref}\right)\frac{\partial\sigma_{out}}{\partial\emptyset_1} + \left(\emptyset_2 - \emptyset_{2\,ref}\right)\frac{\partial\sigma_{out}}{\partial\emptyset_2} + \left(\emptyset_3 - \emptyset_{3\,ref}\right)\frac{\partial\sigma_{out}}{\partial\emptyset_3} + \left(\emptyset_4 - \emptyset_{4\,ref}\right)\frac{\partial\sigma_{out}}{\partial\emptyset_4} \quad (12)$$

$$\emptyset_1 = \left[\frac{Re_{in}}{Re_{in\,ref}}\right]^a, \emptyset_2 = \left[\frac{L_{in}/W_1}{L_{in}/W_{1\,ref}}\right]^b, \emptyset_3 = \left[\frac{W_2/W_1}{W_2/W_{1\,ref}}\right]^c \text{ and } \emptyset_4 = \left[\frac{\emptyset}{\emptyset_{ref}}\right]^d$$

Where $\emptyset_1, \emptyset_2, \emptyset_3$ and $\emptyset_4$ are referred to dimensionless independent groups.

The values of a=4.2, b=1.165, c=0.6 and d=2.0 were determined in order to fit all the trend-lines in a graph and coincide at point $\sigma_{out\,ref}$ =3.7 as shown in Figure 9. The interrelations of dependent variable of σ_{out} with each independent variables were linearized to obtain the best fit straight line.

$$\emptyset_{1\,ref} = \left[\frac{Re_{in\,ref}}{Re_{in\,ref}}\right]^a = 1.0,$$

Therefore, $\emptyset_{2\,ref} = \emptyset_{3\,ref} = \emptyset_{4\,ref} = 1.0$ as well. $\frac{\partial C_p}{\partial\emptyset_1} = 0.0674$, $\frac{\partial C_p}{\partial\emptyset_2}$ =-0.0885, $\frac{\partial C_p}{\partial\emptyset_3} = -0.344$, and $\frac{\partial C_p}{\partial\emptyset_4}$ =0.4275 represented the slopes of the corresponding lines.

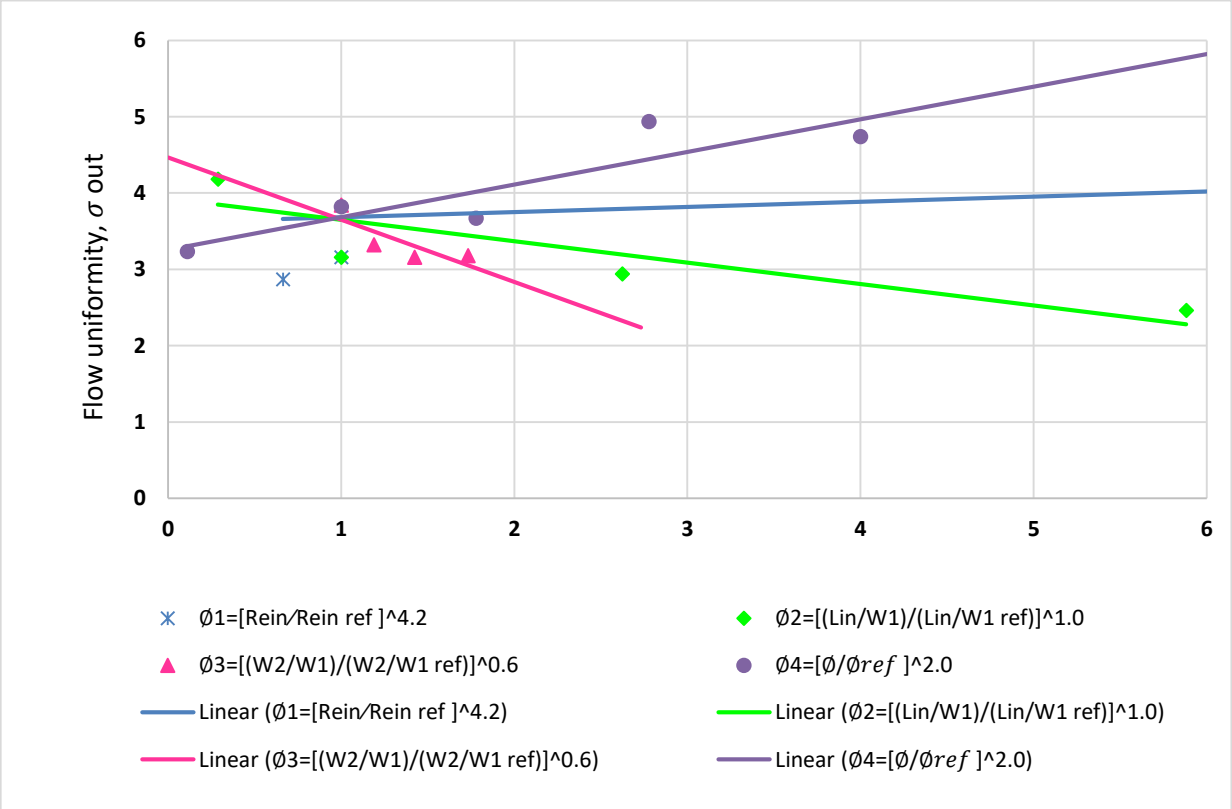

Fig. 9. Flow uniformity index, σ_{out} of 2-D turning diffuser relatives to $\emptyset_1 = [\mathrm{Re_{in}/Re_{in\,ref}}]^{4.2}, \emptyset_2 = [\mathrm{L_{in}/W_1/L_{in}/W_{1\,ref}}]^{1.165}, \emptyset_3 = [\mathrm{W_2/W_1/W_2/W_{1\,ref}}]^{0.6}$ and $\emptyset_4 = [\emptyset/\emptyset_{\mathrm{ref}}]^{2.0}$

All the constraints obtained are substituted into Eq. (12) yielding,

$$\sigma_{out\ acfd} = 3.7 + \left(\left[\frac{Re_{in}}{Re_{in\ ref}}\right]^{4.2} - 1\right)0.0674 - \left(\left[\frac{L_{in}/W_1}{L_{in}/W_{1\ ref}}\right]^{1.165} - 1\right)0.0885 - \left(\left[\frac{W_2/W_1}{W_2/W_{1\ ref}}\right]^{0.6} - 1\right)0.344 + \left(\left[\frac{\emptyset}{\emptyset_{ref}}\right]^{2.0} - 1\right)0.4275 \quad (13)$$

Where,

$Re_{in\ ref} = 6.382 \times 10^4$, $L_{in}/W_{1\ ref}$ = 4.37, $W_2/W_{1\ ref}$ = 1.2 and $\emptyset_{ref} = 90^{\circ}$

ACFD correlations for 2-D curved diffuser to determine pressure recovery, C_p and flow uniformity σ_{out} with acceptable deviation between ACFD, CFD and experimental results were developed. Table 8 shows the deviations of performance correlations.

Table 8
Deviations of performance correlations

Correlation	$C_{p\ acfd}$	$\sigma_{out\ acfd}$
Deviation from experiment (%)	4.16	15.34
Deviation from CFD (%)	18.40	11.23

4. Conclusion

The effect of angle of turn on 2-D curved diffuser was successfully studied. The angle of turn of 2-D curved diffuser is proven to significantly reduce pressure recovery coefficient and increase flow uniformity distortion. The performance correlations in terms of pressure recovery, C_p and flow uniformity, σ_{out} have been developed. The ACFD correlations results show acceptable deviations to CFD and experimental thus reliable to be used to evaluate the performance of 2-D curved diffuser.

Acknowledgement
This research was supported in part by Universiti Tun Hussein Onn Malaysia under TIER1 Vote H172. CFD work was carried out in CFD Laboratory, Universiti Tun Hussein Onn Malaysia (UTHM).

References
[1] Gopaliya, Manoj Kumar, Piyush Goel, Sunil Prashar, and Anil Dutt. "CFD analysis of performance characteristics of S-shaped diffusers with combined horizontal and vertical offsets." *Computers & fluids* 40, no. 1 (2011): 280-290. https://doi.org/10.1016/j.compfluid.2010.09.027
[2] Nordin, Normayati. "Performance investigation of turning diffusers at various geometrical and operating parameters." PhD diss., Universiti Teknologi PETRONAS (UTP), 2016. http://dx.doi.org/10.13140/RG.2.2.33037.13286
[3] Zuan, A. M. S., A. Ruwaidab, S. Syahrullailc, and M. N. Musad. "The Effect of Adding Diffuser by Experimental." *Journal of Advanced Research in Applied Mechanics* 14, no. 1 (2015): 18-24.
[4] Gan, Guohui, and Saffa B. Riffat. "Measurement and computational fluid dynamics prediction of diffuser pressure-loss coefficient." *Applied energy* 54, no. 2 (1996): 181-195. https://doi.org/10.1016/0306-2619(95)00078-X
[5] Schut, S. B., E. H. Van Der Meer, J. F. Davidson, and R. B. Thorpe. "Gas–solids flow in the diffuser of a circulating fluidised bed riser." *Powder Technology* 111, no. 1-2 (2000): 94-103. https://doi.org/10.1016/S0032-5910(00)00245-X
[6] Deniz, Sabri. "Effects of Inlet Flow Field Conditions on the Stall Onset of Centrifugal Compressor Vaned Diffusers." In *ASME International Mechanical Engineering Congress and Exposition*, vol. 37254, pp. 61-74. 2003.

https://doi.org/10.1115/IMECE2003-55221
[7] Cerantola, David. "Evaluation of Swirl and Tabs in Short Annular Diffusers." PhD diss., Queen's University, 2014.
[8] Vaz, Jerson RP, Alexandre LA Mesquita, André L. Amarante Mesquita, Taygoara Felamingo de Oliveira, and Antonio Cesar Pinho Brasil Junior. "Powertrain assessment of wind and hydrokinetic turbines with diffusers." *Energy Conversion and Management* 195 (2019): 1012-1021. https://doi.org/10.1016/j.enconman.2019.05.050
[9] Lindgren, Björn, and Arne V. Johansson. "Design and evaluation of a low-speed wind-tunnel with expanding corners." *Flow Facility Design and Experimental Studies of Wall-Bounded Turbulent Shear-Flows* 63 (2002).
[10] Calautit, John Kaiser, Hassam Nasarullah Chaudhry, Ben Richard Hughes, and Lik Fang Sim. "A validated design methodology for a closed-loop subsonic wind tunnel." *Journal of Wind Engineering and Industrial Aerodynamics* 125 (2014): 180-194. https://doi.org/10.1016/j.jweia.2013.12.010
[11] Fox, Robert W., and S. J. Kline. "Flow regimes in curved subsonic diffusers." *Journal of Basic Engineering* 84, no. 3 (1962): 303-312. https://doi.org/10.1115/1.3657307
[12] Khong, Y. T., N. Nordin, S. M. Seri, A. N. Mohammed, A. Sapit, I. Taib, K. Abdullah, A. Sadikin, and M. A. Razali. "Effect of turning angle on performance of 2-D turning diffuser via Asymptotic Computational Fluid Dynamics." In *IOP Conference Series: Materials Science and Engineering*, vol. 243, no. 1, p. 012013. 2017. http://dx.doi.org/10.1088/1757-899X/243/1/012013
[13] Sparrow, E. M., J. P. Abraham, and W. J. Minkowycz. "Flow separation in a diverging conical duct: Effect of Reynolds number and divergence angle." *International Journal of Heat and Mass Transfer* 52, no. 13-14 (2009): 3079-3083. https://doi.org/10.1016/j.ijheatmasstransfer.2009.02.010
[14] Nordin, Normayati, Zainal Ambri Abdul Karim, Safiah Othman, and Vijay R. Raghavan. "The performance of turning diffusers at various inlet conditions." In *Applied Mechanics and Materials*, vol. 465, pp. 597-602. Trans Tech Publications Ltd, 2014. https://doi.org/10.4028/www.scientific.net/AMM.465-466.597
[15] Huang, Lim Gim, Normayati Nordin, Lim Chia Chun, Nur Shafiqah Abdul Rahim, Shamsuri Mohamed Rasidi, and Muhammad Zahid Firdaus Shariff. "Effect of Turbulence Intensity on Turning Diffuser Performance at Various Angle of Turns." *CFD Letters* 12, no. 1 (2020): 48-61.
[16] Balaji, C., and H. Herwig. "The use of ACFD approach problems involving surface radiation and free convection." *International communications in heat and mass transfer* 30, no. 2 (2003): 251-259. https://doi.org/10.1016/S0735-1933(03)00036-8